

Electrochimica Acta

Effect of Loading Methods on the Performance of Hierarchical Porous Carbon/sulfur Composites in Lithium Sulfur Batteries

--Manuscript Draft--

Manuscript Number:	EA21-1460R
Article Type:	Research Paper
Keywords:	lithium-sulfur battery; sulfur loading methods; hierarchically porous carbon; microporous; mesoporous
Corresponding Author:	Bo Zhang, Ph.D Tianjin Normal University Tianjin, CHINA
First Author:	Bo Zhang, Ph.D
Order of Authors:	Bo Zhang, Ph.D Zhijie Guo Yingming Zhao Birong Luo Dejun Li Teng Zhao Jagadeesh Sure Sri Maha Vishnu Amr Abdelkader Chris Harris Kai Xi
Abstract:	<p>Lithium-sulfur batteries have shown increasing promise for high energy densities and reduced costs. Facile sulfur loading techniques demonstrate a critical way to achieving high dispersions of sulfur in the host's matrix, improving conductivity and simultaneously decreasing the active mass loss from the cathode. Here we investigate the effect of sulfur loading methods on the electrochemical performance of porous carbon/sulfur composites containing approximately 70 wt% sulfur. Three different loading techniques are tested, including one-step molten sulfur impregnation (155 °C), two-step molten sulfur impregnation (155 °C + 300 °C) and a sulfur organic solution impregnation, in which the entire microporous volume of carbon is filled by sulfur. It is found that the simple sulfur organic solution impregnation method is the most effective in enhancing the electrochemical performance of the hierarchical porous carbon/sulfur composite cathode in the lithium-sulfur battery system, due to the weaker interaction occurring between the sulfur and microporous carbon. Our work demonstrates the impact of sulfur loading method on the electrochemical performance of lithium-sulfur batteries, which offers new insights into the preparation technology of electrodes.</p>

1 **Effect of Loading Methods on the Performance of Hierarchical**
2
3 **Porous Carbon/sulfur Composites in Lithium Sulfur Batteries**
4
5
6
7

8 Bo Zhang* ^{a, b}, Zhijie Guo ^{a, b}, Yingming Zhao ^{a, b}, Birong Luo^{a, b}, Dejun Li^{a, b}, Teng
9 Zhao ^c, Jagadeesh Sure ^c, Sri Maha Vishnu ^c, Amr Abdelkader ^{c, d}, Chris Harris ^c, Kai
10 Xi*^c
11
12
13
14
15

16 ^aEnergy & Materials Engineering Centre, College of Physics and Materials Science,
17
18 Tianjin Normal University, Tianjin 300387, China.
19
20

21 ^bTianjin International Joint Research Centre of Surface Technology for Energy Storage
22
23 Materials, Tianjin 300387, China
24
25

26 ^cDepartment of Materials Science and Metallurgy, University of Cambridge,
27
28 Cambridge CB3 0FS, United Kingdom
29
30

31 ^dDepartment of Design and Engineering, Faculty of Science & Technology,
32
33 Bournemouth University, Poole, Dorset, BH12 5BB, United Kingdom.
34
35
36
37
38
39
40

41 *Corresponding authors.
42
43

44 E-mail: zhangbo2014@tjnu.edu.cn (B. Zhang); kx210@cam.ac.uk (K. Xi)
45
46
47
48
49
50
51
52
53
54
55
56
57
58
59
60
61
62
63
64
65

1
2
3 **ABSTRACT:** Lithium-sulfur batteries have shown increasing promise for high energy
4
5
6 densities and reduced costs. Facile sulfur loading techniques demonstrate a critical way
7
8
9 to achieving high dispersions of sulfur in the host's matrix, improving conductivity and
10
11
12 simultaneously decreasing the active mass loss from the cathode. Here we investigate
13
14
15 the effect of sulfur loading methods on the electrochemical performance of porous
16
17
18 carbon/sulfur composites containing approximately 70 wt% sulfur. Three different
19
20
21 loading techniques are tested, including one-step molten sulfur impregnation (155 °C),
22
23
24 two-step molten sulfur impregnation (155 °C + 300 °C) and a sulfur organic solution
25
26
27 impregnation, in which the entire microporous volume of carbon is filled by sulfur. It
28
29
30 is found that the simple sulfur organic solution impregnation method is the most
31
32
33 effective in enhancing the electrochemical performance of the hierarchical porous
34
35
36 carbon/sulfur composite cathode in the lithium-sulfur battery system, due to the weaker
37
38
39 interaction occurring between the sulfur and microporous carbon. Our work
40
41
42 demonstrates the impact of sulfur loading method on the electrochemical performance
43
44
45 of lithium-sulfur batteries, which offers new insights into the preparation technology of
46
47
48 electrodes.
49

50 **Keywords:** lithium-sulfur battery, sulfur loading methods, hierarchically porous carbon,
51
52
53 microporous, mesoporous
54
55
56
57

58 **1. Introduction**

59
60
61
62
63
64
65

1 With the increasing demand for efficient energy storage for electric vehicles (EVs),
2
3 portable devices and smart grids applications, rechargeable lithium-sulfur (Li-S)
4
5 batteries represent a promising candidate for future applications. Li-S cells can offer a
6
7 theoretical capacity as high as 1675 mAhg^{-1} for a sulfur electrode by accepting two
8
9 electrons per sulfur atom [1-6]. Moreover, sulfur is cheap, environmentally friendly,
10
11 and abundant in nature [7-9]. Despite the numerous benefits, there are still several
12
13 noticeable problems that need to be solved to realize the commercialization of Li-S
14
15 cells. One of the most demanding challenges is the intrinsically poor electrical
16
17 conductivity of sulfur and its discharge products ($\text{Li}_2\text{S}_2/\text{Li}_2\text{S}$), which can lead to low
18
19 utilization of the electrochemically active materials [2, 10]. The electrodes also suffer
20
21 from low mechanical and cyclic stability as a result of the volume change of sulfur
22
23 (approximately 80%) during the charge/discharge processes [11, 12]. Another major
24
25 hurdle is the dissolution and diffusion of intermediate polysulfides (Li_2S_n , where $4 \leq n \leq 8$)
26
27 into organic electrolytes [13-15]. Polysulfides can react with the lithium electrodes,
28
29 causing significant active mass loss and severe self-discharging problem [16, 17].
30
31 Continuous reactions between polysulfides and Li anodes restrain their re-oxidation
32
33 to elemental sulfur at the cathode side during the delithiation step [18, 19]. This is
34
35 widely known as a “shuttle” phenomenon in Li-S systems and is considered as one of
36
37 the main reasons for low coulombic efficiency and poor cycling performance [15, 20-
38
39 22].
40
41
42
43
44
45
46
47
48
49
50
51
52
53

54 In order to address the above-mentioned challenges, research has taken two major
55
56 routes: modifying the organic electrolyte to reduce the parasitic reactions with the
57
58
59
60

1 electrodes and replacing sulfur with composites and hybrids that are more conductive
2
3 and more able to accommodate the volume changes [23]. Encapsulating sulfur into a
4
5
6 conductive matrix has been demonstrated to be an effective mean to confine polysulfide
7
8
9 species and improve the electrical conductivity of the electrode [22]. Various
10
11
12 conductive matrixes have been explored, including porous carbon [24-26], carbon
13
14
15 nanotubes [27], carbon nanofibers [28, 29], graphene [30, 31] and graphene derivatives
16
17 [32], metal organic frameworks (MOFs) [33-36] and metal oxides [37-39]. Of particular
18
19
20 interest, porous carbon materials, which include micropores (<2 nm) carbon, mesopores
21
22
23 (2-50 nm) carbon and macropores (>50 nm) carbon, are attractive candidates due to
24
25
26 their low cost and good performance in electrochemical devices. Nazar et al. [40]
27
28
29 reported that highly ordered mesoporous carbon (CMK-3) with an average pore size of
30
31
32 3.33 nm could host S and improve the cycling performance of the sulfur cathode.
33
34
35 However, mesopores in the carbon materials appeared to alleviate but not eliminate the
36
37
38 "shuttle" phenomenon due to the relatively large pore size, which leads to the exposure
39
40
41 of sulfur to the electrolyte [6]. Zhang et al. [41] introduced a sulfur composite with
42
43
44 good cycle stability by confining sulfur in microporous carbon spheres with a narrow
45
46
47 pore size of approximately 0.7 nm. Guo et al. [42] proposed S₂ and S₄ could exist in a
48
49
50 microporous carbon matrix with a pore size of 0.5 nm, which can prevent the
51
52
53 unfavorable cyclo-S₈ to S₄²⁻ transition reactions. Therefore, it is becoming more
54
55
56 convincing that nanoporous carbon can effectively improve the cyclic stability of the
57
58
59 sulfur electrode [26, 43, 44]. However, there is no systemic study of the effect of sulfur
60
61
62 loading method on the electrochemical performance of hierarchical porous carbon-

1 sulfur composites.

2
3 In this study, we have selected polypyrrole as a precursor to synthesize hierarchical
4 porous carbon (HPC) model materials. HPC produced from polypyrrole precursors has
5 previously shown to have a high microporous volume of $1.3 \text{ cm}^3 \text{ g}^{-1}$, a total pore volume
6 of $2.6 \text{ cm}^3 \text{ g}^{-1}$ and a large (BET) surface area of $3270.4 \text{ m}^2 \text{ g}^{-1}$ [45]. We studied three
7 sulfur loading methods, each of which impacted the state of sulfur within the carbon
8 micropores and affected the electrochemical performance of the sulfur composite
9 significantly. Our study provides an excellent guideline to the selection of optimal
10 sulfur loading method for sulfur cathode with excellent performance.
11
12
13
14
15
16
17
18
19
20
21
22
23
24

25 **2. Experimental section**

26 **2.1. Preparation of microporous/low-range mesoporous carbon**

27
28 The preparation process of the hierarchical porous carbon is illustrated in Fig.1.
29
30 Firstly, Polypyrrole (PPy) was prepared by a simple synthesis route using FeCl_3 as an
31 oxidant [46]. Typically, 5 ml pyrrole was distilled at $120 \text{ }^\circ\text{C}$ to acquire approximately
32 3 ml of product. The distilled pyrrole was then added to a 200 ml solution of 0.5 M
33 FeCl_3 , and the mixture was stirred for 2 hours using magnetic stirring until full
34 polymerization. The resulting polypyrrole was then filtered and washed with water and
35 ethanol before drying in the oven overnight. The dry powder was then mixed with KOH
36 pellets in a 1:4 weight ratio and oven dried at $150 \text{ }^\circ\text{C}$. Chemical activation of the
37 polymer was conducted by heating the PPy-KOH mixture under ultra-high purity argon
38 for 1 hour at $800 \text{ }^\circ\text{C}$ (heating rate: $3 \text{ }^\circ\text{C} \cdot \text{min}^{-1}$). The activated samples were washed with
39 hydrochloric acid (10 wt%) to remove any inorganic salt residue, followed by rinsing
40
41
42
43
44
45
46
47
48
49
50
51
52
53
54
55
56
57
58
59
60
61
62
63
64
65

1 with distilled water until a neutral pH was obtained. Finally, the sample was dried at
2
3
4 120 °C and labelled as HPC.
5

6 **2.2. Preparation of HPC/sulfur composites**

7

8
9 The synthesis procedure of the HPC/S composites is illustrated in Fig.1. The HPC
10 prepared from the previous step was used as the matrix and sublimed sulfur (Aladdin,
11 Shanghai) was used as the sulfur source. We have used three methods to load sulfur into
12 the carbon matrix. In the first method, we used one single heat treatment step in which
13 a mixture of HPC and sublimed sulfur (weight ratio of 1:2.33) was heated at 155 °C for
14 10 h in a sealed reactor under an argon atmosphere. At this temperature, the melted
15 sulfur with low viscosity can quickly diffuse into the micropores of the HPC. The
16 outcome of this process was a 70 wt% sulfur loading, which was designated as HPC/S-
17 155-70%. The second method is a two-step process in which HPC was mixed with
18 sublimed sulfur in a weight ratio of 1:4. The mixture was heated firstly at 155 °C for 6
19 h in a sealed vessel filled with argon gas, and then the temperature was increased to
20 300 °C and held for 2 h in order to vaporize the superfluous sulfur on the surface of the
21 carbon. The sulfur content of the composite was calculated from the mass change before
22 and after heat treatment to be 68 wt%. This composite was designated as HPC/S-300-
23 68%. The third loading method used the same mixing ratio as in the first method (a
24 weight ratio of 1:2.33), but the mixture was dissolved in 50 ml CS₂ solution and stirred
25 vigorously until CS₂ was evaporated entirely using magnetic stirring. A composite with
26 70 wt% sulfur was obtained and designated as HPC/S-Sol-70%. For comparison, the
27 graphene material (PH: 2±0.2; N, S, Cl%<0.5%; metal impurity<100ppm; ash<1.0%)
28
29
30
31
32
33
34
35
36
37
38
39
40
41
42
43
44
45
46
47
48
49
50
51
52
53
54
55
56
57
58
59
60

1 obtained from Inner Mongolia RS new Energy Co., Ltd was incorporated with sulfur
2
3 using the same three methods. And the prepared composites were designated as
4
5 Graphene/S-155, Graphene/S-Sol, Graphene/S-300, respectively, in which sulfur
6
7 contents were all about 50 wt%.
8
9

10 11 **2.3. Materials characterizations**

12
13
14 The HPC and HPC/sulfur composites were characterized using X-ray diffraction
15
16 (XRD, Bruker D8a) with Cu-K α radiation, scanning electron microscopy (SEM,
17
18 SU8010, Hitachi) equipped with energy dispersive spectroscopy (EDS) and
19
20 transmission electron microscopy (TEM, JEOL JEM-3000F). Nitrogen (N₂)
21
22 adsorption/desorption measurements were performed using a Quantachrome
23
24 instrument (Quabrorb SI-3MP) at -196 °C to investigate the porous structure of the
25
26 samples. The sulfur content in the composites was measured using thermogravimetric
27
28 analysis (TGA, Pyris Diamond6000 TG/DTA, PerkinElmer). The electrical
29
30 conductivity of the cathode was determined by four probe measurements at room
31
32 temperature.
33
34
35
36
37
38
39
40
41

42 **2.4. Electrochemical characterizations**

43
44 To prepare the cathode, the HPC/S composite material, carbon black and
45
46 polyvinylidene fluoride (PVDF) binder were mixed in a weight ratio of 70: 20: 10 with
47
48 N-methyl-2-pyrrolidinone (NMP) as a dispersant. Afterwards, the resulting slurry was
49
50 spread onto nickel foam with a 10 mm diameter and dried at 60 °C for 12 h in an oven,
51
52 then compressed into tablets. The areal sulfur loading is approximate 1.5 mg cm⁻², 7
53
54 mg cm⁻² and the electrolyte-to-sulfur mass is about 20 ml g⁻¹. The CR2032-type coin
55
56
57
58
59
60
61
62
63
64
65

1 cells were assembled in an argon-filled glovebox. The electrolyte used was LiTFSI
2
3 (Sigma-Aldrich) in a solvent mixture of 1,3-dioxolane and 1,2-dimethoxyethane (1:1,
4
5 v/v) (Aladdin) with 0.2 M LiNO₃ additive. Lithium chips were used as both the counter
6
7 and reference electrode. Celgard 2400 membranes were used as separators. To evaluate
8
9 the capacity and cycle stability of the electrodes, galvanostatic charge-discharge tests
10
11 were conducted using Arbin Instrument BT2000 model in the voltage range of 1-3 V
12
13 and 1.6-2.8 V. Cyclic voltammogram (CV) measurements were performed using
14
15 Princeton Applied Research instrument in the voltage range of 1-3 V and 1.6-2.8 V with
16
17 a scanning rate of 0.1 mV S⁻¹. The electrochemical impedance spectroscopy (EIS) was
18
19 carried out at an amplitude of 5 mV over the frequency range from 100 kHz to 0.01 Hz.
20
21 All electrochemical characterizations were conducted at ambient temperature.
22
23
24
25
26
27
28
29
30

31 **3. Results and discussion**

32
33 The N₂ adsorption/desorption measurements were employed to investigate the
34
35 porous structure of the HPC and HPC/S composite materials. Fig. 2A ,B show the N₂
36
37 adsorption/desorption isotherm measured at -196 °C for the HPC and HPC/S
38
39 composites. The isotherm shows typical type I behavior, implying the existence of a
40
41 multitude of micropores in HPC[41]. The pore size distribution curve (Fig. 2C)
42
43 confirmed the presence of the micropores peaked at 1.8 nm. Also, the HPC possesses a
44
45 relatively high total pore volume of 2.6 cm³ g⁻¹ and a large (BET) surface area of 3270.4
46
47 m² g⁻¹ based on density functional theory (DFT) calculation, which are created by
48
49 classical approaches to adsorption as well as models based on modern statistical
50
51 thermodynamics. More importantly, the microporous volume of the carbon material is
52
53
54
55
56
57
58
59
60

1 1.3 cm³ g⁻¹, which theoretically could host up to 72% sulfur loading when calculated
2
3 based on the density of sulfur (2.07 g·cm⁻³ for α phase at room temperature)[41].
4
5 Although different sulfur loading methods were conducted in this work, the similar
6
7 sulfur content close to the theoretical value could be obtained. The calculated specific
8
9 surface areas decrease sharply to 128.4, 4.7 and 16.2 m² g⁻¹ for the HPC/S-Sol-70%,
10
11 HPC/S-155-70%, HPC/S-300-68% composite materials, respectively. The reason for
12
13 the relatively larger specific surface and higher pore volume of HPC/S-Sol-70% can be
14
15 explained through the existence of a stretching force between the nanopores and the
16
17 CS₂ solution of sulfur, resulting in a deposition of some sulfur nanocrystals onto the
18
19 surface of HPC[19]. Fig. 3A shows the XRD patterns of sublimed sulfur, HPC and the
20
21 HPC/S composites. For elemental sulfur, characteristic sharp peaks can be observed in
22
23 its XRD pattern, which is coincident with the orthorhombic crystal structure of
24
25 sulfur[47]. The XRD pattern of the HPC shows two broad diffraction peaks at around
26
27 30° and 43°[47, 48], which can be assigned to the diffractions of (002) and (100) planes
28
29 of graphitic carbon (JCPDS No 75-1621). The broadening and low intensity of the
30
31 peaks indicate less crystallinity of the HPC. None of the HPC/S composites, regardless
32
33 of the sulfur loading method, contain the characteristic peaks of crystalline sulfur,
34
35 indicating that the nano-sized sulfur exists in the composite material. Despite nano-
36
37 sized sulfur exists in the composite material, the three cathodes have an electrical
38
39 conductivity of 7–8 S cm⁻¹ at room temperature.
40
41
42
43
44
45
46
47
48
49
50
51
52
53
54
55

56 TGA is a technique used traditionally to determine the thermal stability of the
57
58 materials. When it comes to composites, TGA could also give an idea about the energy
59
60
61
62
63
64
65

1 needed to break the interactions between the components and the composition of the
2 composite. The three HPC/S composites in the current study have almost the same
3 elemental composition. However, looking at their TGA curves in Fig. 3B, one can
4 observe some differences in their response to increasing the temperature. The sulfur in
5 HPC/S-155-70% evaporates at a slightly higher temperature than that in HPC/S-Sol-
6 70%, indicating a stronger interaction between sulfur and carbon. This can be explained
7 by understanding the loading mechanism and the pores structures in both composites.
8 In the HPC/S-155-70% composites, sulfur melts and diffuses into pores that are larger
9 than 0.69 nm in the form of S₈[49]. On the other hand, the sulfur in the HPC/S-Sol-70%
10 composite is introduced to the pores using CS₂ as a flux, which when evaporates, leaves
11 less solid filling inside the nanopores and some sulfur nanocrystals on the surface of
12 HPC. The TGA curve of the HPC/S-300-68% shows an interesting feature. The mass
13 loss above the evaporation temperature of the sulfur is somewhat gradual, suggesting
14 the removal of sulfur is taking place over a wide range of temperature, and by a more
15 complicated mechanism than simple evaporation. This can be explained by the
16 difficulty of evaporating sulfur from the ultramicropores(<0.69nm) in the form of
17 smaller sulfur molecules (S₂₋₄)[42].

18 The SEM images of the polypyrrole (PPy), HPC and the HPC/S composites are
19 shown in Fig. 4. Low and high magnification SEM images of polypyrrole (PPy) shown
20 in Fig. 4A, B exhibit clusters of interconnected microparticles. After the carbonization
21 and activation (Fig. 4C, Fig. S1A), the surface of the HPC became rougher due to the
22 formation of a range of micropores. The SEM images of the HPC/S composites at low

1 magnification (Fig. 4D, E, F) and high magnification (Fig. S1B, C, D) show that there
2
3 is no discernible morphological difference after loading HPC with sulfur. SEM images
4
5 are also pointing out that the morphology of HPC/S composites is independent of sulfur
6
7 loading method. Fig. 5 shows TEM images of the HPC (Fig. 5A) and the HPC/S
8
9 composites (Fig. 5B, C). The TEM image (Fig. 5D) and EDX point analysis result (Fig.
10
11 S7) of the HPC/S-Sol-70% confirms the deposition of 5 nm sulfur particles on the
12
13 surface of HPC. Elemental mapping results of three HPC/S composites are shown in
14
15 Fig.5E to G in which the sulfur (yellow) map is almost in full accordance with the
16
17 carbon (purple) map. These results further confirm that sulfur is homogeneously
18
19 dispersed in the carbon matrix.
20
21
22
23
24
25
26
27

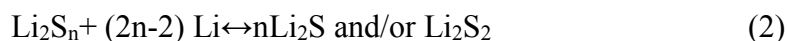
28 In order to understand the effect of the sulfur loading method on the
29
30 electrochemical performance, the cycling performances of the HPC/S composites at
31
32 200mA/g were tested. HPC/S-155-70% and HPC/S-Sol-70% show higher capacity and
33
34 more stable circulation than that of HPC/S-300-68%. HPC-155-70% and HPC/S-Sol-
35
36 70% are generally “open-type” composites, meaning free S₈ exist both in pores larger
37
38 than 0.69 nm. In this way, sulfur can contact directly to electrolyte solvents and become
39
40 electrochemically active[49]. HPC/S-300-68%, on the other hand, has a less open
41
42 structure, with pores size less than 0.69 nm. The electrochemical behavior of HPC/S-
43
44 300-68% appears to be significantly different from the other two composites (Fig. 6).
45
46 During the initial cycle, all sulfur in the form of S₂₋₄ infiltrates into micropores, leading
47
48 to discharge potential hysteresis[41, 42, 53, 54] and exhibit only one shoulder peak at
49
50 1.53 V. During subsequent cycles, the cathodic peak potential shifts to about 1.42 V
51
52
53
54
55
56
57
58
59
60

1 (Fig. S2). There is a broad anodic peak at approximately 2.26 V with low peak current,
2
3 implying severe polarization of the electrode and the poor charge capacity. This is
4
5 related to the reduction of all the smaller sulfur molecules confined within the
6
7 microporous (<0.69 nm) carbon, which is required to overcome the absorption energy.
8
9 Also, the reactive and large surface area of carbon exposed to the electrolyte causes a
10
11 large irreversible capacity[55]. Solvent molecules can also be blocked by
12
13 micropores.[56] Thus, it is essential for any electrode material to have a larger pores
14
15 volume and/or a significant amount of mesopores to facilitate the transport of Li⁺ ions.
16
17 The CV results showed the critical role of the loading methods on the electrochemical
18
19 performance of sulfur-HPC electrode by changing both the morphology and the
20
21 condition of the sulfur existing within the electrode.
22
23
24
25
26
27
28
29

30 The interfacial properties of the three materials were further studied by the
31
32 electrochemical impedance spectroscopy (EIS). Fig. S3 shows the Nyquist plots of the
33
34 three HPC/S composites, which are all composed of a semicircle at high frequency and
35
36 an inclined line in the low-frequency region. These features represent the charge
37
38 transfer resistances between electrolyte and electrode and the resistance of lithium ion
39
40 diffusion into the active mass, respectively[58]. In addition, the intercept at the real Z
41
42 axis corresponds to the sum resistance, which includes the ionic conductivity of the
43
44 electrolyte, the inherent resistance of the cathode, anode, separator, the interphase
45
46 electronic contact resistance on the cathode, and the interfacial resistance of the lithium
47
48 anode[58, 59]. As expected, HPC/S-300-68% exhibits the highest charge transfer
49
50 resistance (88.56 Ω), due to all the smaller sulfur molecules confined within the
51
52
53
54
55
56
57
58
59
60

1 microporous (<0.69 nm) carbon, resulting in blocking electrolyte contact directly to S.
2
3 On the contrary, HPC/S-Sol-70% and HPC/S-300-68% exhibits almost transfer
4
5 resistance. This can be explained by the fact that sulfur exists in pores larger than 0.69
6
7 nm on the surface of the porous carbon , which makes sulfur easily accessible by the
8
9 electrolyte, leading to lower charge transfer resistances.
10
11
12

13
14 HPC/S-155-70% and HPC/S-Sol-70% were studied in detail below to further
15
16 understand the effect of the sulfur loading method on the electrochemical performance.
17
18 Cyclic voltammetry (CV) methods were conducted for HPC/S-155-70% and HPC/S-
19
20 Sol-70%. The CV curves of the initial three cycles of the two HPC/S composite cathodes
21
22 are shown in Fig. 7A, B which was recorded between 1.6-2.8 V. It could be observed
23
24 that there are two sharp peaks at 2.3 and 2.03 V, corresponding to the two-step reduction
25
26 in the initial cathodic process of HPC/S-Sol-70%. The peak at 2.3 V can be attributed
27
28 to the reduction of elemental sulfur into long-chain lithium polysulfides (Li_2S_n) ($4 \leq n$
29
30 ≤ 8) and the other cathodic peak at 2.03 V is typically associated with the conversion
31
32 reaction of the polysulfides anions into short-chain lithium sulfides (Li_2S and/or
33
34 Li_2S_2)[50, 51].
35
36
37
38
39
40
41
42
43



44
45
46
47 In the anodic scan, there are two peaks at 2.37, 2.42 V, which can be attributed to
48
49 the conversion of $\text{Li}_2\text{S}_2/\text{Li}_2\text{S}$ into high-order polysulfides and S[52]. The intensity of
50
51 the reduction peaks decreases slightly with subsequent cycling. There is almost no
52
53 change from the 2nd cycle onwards, indicating relatively good reversibility. With
54
55
56
57
58
59
60

1 regards to the CV profile of HPC/S-155-70%, the first two cathodic and anodic peaks
2
3 are similar to those observed in HPC/S-Sol-70%, indicating the same discharge process.
4
5

6 We have then used the charge/discharge method to further study the electrochemical
7
8 behavior of the sulfur-HPC composites as electrodes for Li-S batteries. Fig. 7C, D
9 shows the charge/discharge voltage profiles of the HPC/S-Sol-70% , HPC/S-155-70%
10 at first cycle of various C rates from 0.1C to 2 C. There are two voltage plateaus can be
11 observed during the discharge process at around 2.3 and 2.1 V for the HPC/S-Sol -70%,
12 HPC/S-155-70%, which is in good agreement with the corresponding CV profile.
13
14 During the charging process, one plateau of the HPC/S composite cathode also
15 corresponds to the oxidation reaction shown in the CV curve. Furthermore, the HPC/S-
16 Sol-70% showed lower voltage hysteresis ($\Delta E=175\text{mV}$) than that of HPC/S-155-70%
17 ($\Delta E=200\text{mV}$) due to sulfur can contact directly to electrolyte solvents and become
18 electrochemically active implying greater electrochemical kinetics
19
20
21
22
23
24
25
26
27
28
29
30
31
32
33
34
35

36 The rate performances of the two composite cathodes were further investigated at
37 various current densities from 0.1C to 2C. As can be seen from Fig. 8A, HPC/S-Sol-
38 70% delivers reversible capacities of 1324.5, 778.9, 732.3, 663.5, 593.5 mAh g⁻¹ at
39 current densities of 0.1 C, 0.3 C, 0.5 C, 1 C, 2 C respectively, which are much higher
40 than those of other HPC/composites. When the current density is returned to 0.1C, the
41 capacity is recovered to values of 809.5, 803.5 mAh g⁻¹, for the HPC/S-Sol-70%,
42 HPC/S-155-70% composites, respectively. This again shows how the pore structures
43 formed by the solvent-mediated loading method facilitated the utilization of sulfur. The
44 cycling performances of the two composites over 300 cycles at 1C between 1.6-2.8 V
45
46
47
48
49
50
51
52
53
54
55
56
57
58
59
60

1 are shown in Fig. 8B. After 300 cycles, the discharge capacities of the two samples
2 reach 599, 578.8 mAh g⁻¹ for HPC/S-Sol-70%, HPC/S-155-70% respectively. The
3 HPC/S-Sol-70% composite cathode exhibited a better cycling performance, implying
4 that the simple wet chemical synthesis route of deposition method contributes to a
5 significant restriction of the shuttle effect for polysulfides. After 100 cycles, the
6 morphology of the positive electrode was tested. Compared with before cycling, there
7 is little difference, and there is no large sulfur deposit (Fig. S4). Additionally, the
8 HPC/S-Sol-70% composite cathode with 7 mg cm⁻² sulfur areal loading also exhibited
9 a high areal capacity of 8.7 mAh cm⁻² at a current density of 0.1 C and maintained a
10 high areal capacity of 4.45 mAh cm⁻² at a current density of 0.2 C after 98 cycles (Fig.
11 8b, Fig. S5).

12 The role of the loading method in enhancing the electrochemical performance of
13 carbon-sulfur composites is not limited to HPC. We have conducted a series of
14 controlled experiments as a proof of concept with other carbon nanomaterials. Figure
15 S6 showed the performance of graphene-based electrodes loaded with sulfur using
16 similar methods to that used with HPC, i.e, single step heating at 150 °C, two-steps heat
17 treatment at 150 °C and 300°C, and finally solution-mediated loading. The electrodes
18 prepared by loading sulfur from organic solvents have the highest initial and subsequent
19 capacity. Numerically, graphene/S-Sol electrode showed an initial capacity of about
20 1160 mAh g⁻¹ and 815 mAh g⁻¹ in the second cycle and dropped to 330 mAh g⁻¹ after
21 100 cycles. The graphene sample heated in sulfur at 150 °C has an initial capacity of
22 1045 mAh g⁻¹ and maintained a capacity of ~ 250 mAh g⁻¹ after 100 cycles. While both

1 the capacity and the cyclability are less than those of HPC, it is clear that using organic
2
3 solvent as a flux to load the sulfur on/in the carbon matrix significantly improve the
4
5 performance of the electrodes. The hierarchical porosity of HPC enhances the
6
7 performance further by restricting the parasitic reactions.
8
9

10 11 **4. Conclusions**

12
13 In summary, hierarchical porous carbon (HPC) with good electrical conductivity,
14
15 high specific surface area and large micro- and low-range mesoporous volume has been
16
17 derived from a polypyrrole precursor. When comparing three different sulfur loading
18
19 methods, it was observed that each method has a significant effect on the state of sulfur
20
21 existing on the carbon, and influences the electrochemical performance of the HPC/S
22
23 composite cathode. For the “two-step molten sulfur impregnation” method, all the
24
25 smaller sulfur molecules are confined within the microporous (< 0.69 nm) carbon (from
26
27 S_{2-4} to Li_2S), causing the electrochemical reaction needs to overcome high absorption
28
29 energy. The solvent molecules can also be blocked by the micropores, thus, the carbon
30
31 needs far more mesopores or macropores to facilitate the transport of solvent and
32
33 lithium ions. The “one-step molten sulfur impregnation” method produced a composite
34
35 that slows down the electrochemical reaction due to the need to overcome a strong
36
37 interaction during the discharge process. However, a sulfur organic solution
38
39 impregnation method ensures that sulfur is well dispersed inside the micropores (> 0.69
40
41 nm) without strong interaction between sulfur and micropores. In addition, the sulfur
42
43 within the micropores of the HPC/S-Sol-70% composite exposed to the electrolyte
44
45 becomes electrochemically active, accompanied by the strong adsorbing ability for
46
47
48
49
50
51
52
53
54
55
56
57
58
59
60
61
62
63
64
65

1 polysulfides by HPC material. These factors contribute to the excellent electrochemical
2
3 performance of the composite cathode. In order to demonstrate the universality of the
4
5 conclusion, we also prepared graphene/sulfur composites with three loading methods.
6
7
8 Their performances showed the same results. Therefore, this work can assist in
9
10 designing an optimal sulfur loading method for sulfur cathode with excellent
11
12 performance.
13
14
15

16 **Acknowledgment**

17
18 This work was financially supported by R&D project (0620301- 53H16023) for Li
19
20 batteries by Anshan Xingde Material Technology Corporation.
21
22
23

24 **References**

- 25
26
27
28 [1] P.G. Bruce, S.A. Freunberger, L.J. Hardwick, J.-M. Tarascon, *Nature materials*, 11 (2011)
29
30 172-172.
31
32
33 [2] K. Cai, M.K. Song, E.J. Cairns, Y. Zhang, *Nano letters*, 12 (2012) 6474-6479.
34
35
36 [3] Y. Fu, Y.S. Su, A. Manthiram, *Angewandte Chemie*, 52 (2013) 6930-6935.
37
38
39 [4] A. Manthiram, S.H. Chung, C. Zu, *Advanced materials*, 27 (2015) 1980-2006.
40
41
42 [5] A. Rosenman, E. Markevich, G. Salitra, D. Aurbach, A. Garsuch, F.F. Chesneau, *Advanced*
43
44 *Energy Materials*, 5 (2015) 1500212.
45
46
47 [6] Y.X. Yin, S. Xin, Y.G. Guo, L.J. Wan, *Angewandte Chemie*, 52 (2013) 13186-13200.
48
49
50 [7] S.H. Chung, A. Manthiram, *Advanced materials*, 26 (2014) 1360-1365.
51
52
53 [8] B. Ding, C. Yuan, L. Shen, G. Xu, P. Nie, X. Zhang, *Chemistry*, 19 (2013) 1013-1019.
54
55
56 [9] R. Elazari, G. Salitra, A. Garsuch, A. Panchenko, D. Aurbach, *Advanced materials*, 23
57
58 (2011) 5641-5644.
59
60

- 1 [10] Z. Dong, J. Zhang, X. Zhao, J. Tu, Q. Su, G. Du, RSC Advances, 3 (2013) 24914.
2
3
4 [11] K.E. Hendrickson, L. Ma, G. Cohn, Y. Lu, L.A. Archer, Advanced science, 2 (2015)
5
6 1500068.
7
8
9 [12] S.C. Jung, Y.-K. Han, Journal of Power Sources, 325 (2016) 495-500.
10
11
12 [13] C. Barchasz, J.-C. Leprêtre, F. Alloin, S. Patoux, Journal of Power Sources, 199 (2012)
13
14 322-330.
15
16
17 [14] S. Evers, T. Yim, L.F. Nazar, The Journal of Physical Chemistry C, 116 (2012) 19653-
18
19 19658.
20
21
22 [15] R. Xu, I. Belharouak, J.C.M. Li, X. Zhang, I. Bloom, J. Bareño, Advanced Energy Materials,
23
24 3 (2013) 833-838.
25
26
27 [16] N. Jayaprakash, J. Shen, S.S. Moganty, A. Corona, L.A. Archer, Angewandte Chemie, 50
28
29 (2011) 5904-5908.
30
31
32 [17] X. Ji, S. Evers, R. Black, L.F. Nazar, Nature communications, 2 (2011) 325.
33
34
35
36 [18] J.Y. Koh, S. Kim, M.-S. Park, H.J. Yang, T.H. Yang, Y. Jung, Electrochimica Acta, 212
37
38 (2016) 212-216.
39
40
41 [19] C. Liang, N.J. Dudney, J.Y. Howe, Chemistry of Materials, 21 (2009) 4724-4730.
42
43
44 [20] G. Xu, B. Ding, L. Shen, P. Nie, J. Han, X. Zhang, Journal of Materials Chemistry A, 1
45
46 (2013) 4490.
47
48
49 [21] Y. Xu, Y. Wen, Y. Zhu, K. Gaskell, K.A. Cychosz, B. Eichhorn, K. Xu, C. Wang, Advanced
50
51 Functional Materials, 25 (2015) 4312-4320.
52
53
54 [22] Y. Yang, G. Zheng, Y. Cui, Chemical Society reviews, 42 (2013) 3018-3032.
55
56
57 [23] V.C. Hoang, V. Do, I.W. Nah, C. Lee, W.I. Cho, I.H. Oh, Electrochimica Acta, 210 (2016)
58
59

1-6.

[24] S.-R. Chen, Y.-P. Zhai, G.-L. Xu, Y.-X. Jiang, D.-Y. Zhao, J.-T. Li, L. Huang, S.-G. Sun,
Electrochimica Acta, 56 (2011) 9549-9555.

[25] D.S. Jung, T.H. Hwang, J.H. Lee, H.Y. Koo, R.A. Shakoor, R. Kahraman, Y.N. Jo, M.S.
Park, J.W. Choi, Nano letters, 14 (2014) 4418-4425.

[26] J. Schuster, G. He, B. Mandlmeier, T. Yim, K.T. Lee, T. Bein, L.F. Nazar, Angewandte
Chemie, 51 (2012) 3591-3595.

[27] X.Z. Ma, B. Jin, P.M. Xin, H.H. Wang, Applied Surface Science, 307 (2014) 346-350.

[28] G. Zheng, Y. Yang, J.J. Cha, S.S. Hong, Y. Cui, Nano letters, 11 (2011) 4462-4467.

[29] G. Zheng, Q. Zhang, J.J. Cha, Y. Yang, W. Li, Z.W. Seh, Y. Cui, Nano letters, 13 (2013)
1265-1270.

[30] L. Ji, M. Rao, H. Zheng, L. Zhang, Y. Li, W. Duan, J. Guo, E.J. Cairns, Y. Zhang, Journal
of the American Chemical Society, 133 (2011) 18522-18525.

[31] H. Wang, Y. Yang, Y. Liang, J.T. Robinson, Y. Li, A. Jackson, Y. Cui, H. Dai, Nano letters,
11 (2011) 2644-2647.

[32] N. Li, M. Zheng, H. Lu, Z. Hu, C. Shen, X. Chang, G. Ji, J. Cao, Y. Shi, Chemical
communications, 48 (2012) 4106-4108.

[33] H.B. Wu, S. Wei, L. Zhang, R. Xu, H.H. Hng, X.W. Lou, Chemistry, 19 (2013) 10804-10808.

[34] K. Xi, S. Cao, X. Peng, C. Ducati, R.V. Kumar, A.K. Cheetham, Chemical communications,
49 (2013) 2192-2194.

[35] C. Zha, D. Wu, T. Zhang, J. Wu, H. Chen, Energy Storage Materials, 17 (2019) 118-125.

[36] C. Zha, F. Yang, J. Zhang, T. Zhang, S. Dong, H. Chen, Journal of Materials Chemistry A,

1 6 (2018) 16574-16582.

2
3 [37] K.T. Lee, R. Black, T. Yim, X. Ji, L.F. Nazar, *Advanced Energy Materials*, 2 (2012) 1490-
4
5 1496.

6
7
8 [38] X. Liang, C.Y. Kwok, F. Lodi-Marzano, Q. Pang, M. Cuisinier, H. Huang, C.J. Hart, D.
9
10 Houtarde, K. Kaup, H. Sommer, T. Brezesinski, J. Janek, L.F. Nazar, *Advanced Energy*
11
12 *Materials*, 6 (2016) 1501636.

13
14
15 [39] Z. Wei Seh, W. Li, J.J. Cha, G. Zheng, Y. Yang, M.T. McDowell, P.C. Hsu, Y. Cui, *Nature*
16
17 *communications*, 4 (2013) 1331.

18
19
20 [40] X. Ji, K.T. Lee, L.F. Nazar, *Nature materials*, 8 (2009) 500-506.

21
22
23 [41] B. Zhang, X. Qin, G.R. Li, X.P. Gao, *Energy & Environmental Science*, 3 (2010) 1531.

24
25
26 [42] S. Xin, L. Gu, N.H. Zhao, Y.X. Yin, L.J. Zhou, Y.G. Guo, L.J. Wan, *Journal of the American*
27
28 *Chemical Society*, 134 (2012) 18510-18513.

29
30
31 [43] S. Niu, G. Zhou, W. Lv, H. Shi, C. Luo, Y. He, B. Li, Q.-H. Yang, F. Kang, *Carbon*, 109
32
33 (2016) 1-6.

34
35
36 [44] J. Song, T. Xu, M.L. Gordin, P. Zhu, D. Lv, Y.-B. Jiang, Y. Chen, Y. Duan, D. Wang,
37
38 *Advanced Functional Materials*, 24 (2014) 1243-1250.

39
40
41 [45] Z. Guo, B. Zhang, D. Li, T. Zhao, P.R. Coxon, C.J. Harris, R. Hao, Y. Liu, K. Xi, X. Li,
42
43 *Electrochimica Acta*, 230 (2017) 181-188.

44
45
46 [46] M. Sevilla, P. Valle-Vigón, A.B. Fuertes, *Advanced Functional Materials*, 21 (2011) 2781-
47
48 2787.

49
50
51 [47] K. Balakumar, R. Sathish, N. Kalaiselvi, *Electrochimica Acta*, (2016).

52
53
54 [48] G.C. Li, J.J. Hu, G.R. Li, S.H. Ye, X.P. Gao, *Journal of Power Sources*, 240 (2013) 598-
55
56

1 605.

2
3 [49] Z. Li, L. Yuan, Z. Yi, Y. Sun, Y. Liu, Y. Jiang, Y. Shen, Y. Xin, Z. Zhang, Y. Huang, *Advanced*
4
5
6 *Energy Materials*, 4 (2014) 1301473.

7
8
9 [50] Y. Fu, A. Manthiram, *RSC Advances*, 2 (2012) 5927.

10
11 [51] D. Wang, A. Fu, H. Li, Y. Wang, P. Guo, J. Liu, X.S. Zhao, *Journal of Power Sources*, 285
12
13 (2015) 469-477.

14
15 [52] L.-X. Miao, W.-K. Wang, A.-B. Wang, K.-G. Yuan, Y.-S. Yang, *Journal of Materials*
16
17
18
19
20 *Chemistry A*, 1 (2013) 11659.

21
22 [53] K. Xi, P.R. Kidambi, R. Chen, C. Gao, X. Peng, C. Ducati, S. Hofmann, R.V. Kumar,
23
24
25
26 *Nanoscale*, 6 (2014) 5746-5753.

27
28 [54] D.W. Wang, G. Zhou, F. Li, K.H. Wu, G.Q. Lu, H.M. Cheng, I.R. Gentle, *Physical chemistry*
29
30
31 *chemical physics : PCCP*, 14 (2012) 8703-8710.

32
33 [55] J. Kim, D.-J. Lee, H.-G. Jung, Y.-K. Sun, J. Hassoun, B. Scrosati, *Advanced Functional*
34
35
36
37 *Materials*, 23 (2013) 1076-1080.

38
39 [56] D.-W. Wang, Q. Zeng, G. Zhou, L. Yin, F. Li, H.-M. Cheng, I.R. Gentle, G.Q.M. Lu, *Journal*
40
41
42
43 *of Materials Chemistry A*, 1 (2013) 9382.

44
45 [57] S.S. Zhang, *Electrochimica Acta*, 70 (2012) 344-348.

46
47 [58] Z. Zhang, Y. Lai, Z. Zhang, K. Zhang, J. Li, *Electrochimica Acta*, 129 (2014) 55-61.

48
49
50 [59] W. Zhou, X. Xiao, M. Cai, L. Yang, *Nano letters*, 14 (2014) 5250-5256.

51
52
53
54
55
56 **Figure captions:**

57
58 **Fig. 1.** Schematic of the synthesis procedure of HPC and HPC/S.

1 **Fig. 2.** Nitrogen adsorption/desorption isotherms of microporous/low-range
2 mesoporous carbon hierarchical porous carbons (HPC) (A), the HPC/S composites (B)
3 at -196 °C. The pore distributions of HPC (C) and the HPC/S (D).

4
5
6
7
8
9 **Fig. 3.** (A) XRD patterns of HPC, HPC/S composites and sulfur. (B) TGA curves of the
10 as-prepared HPC/S composites recorded under argon atmosphere with a heating rate of
11 10 °C min⁻¹.

12
13
14
15
16
17 **Fig. 4.** SEM images of polypyrrole(PPy) (A, B), HPC (C), HPC/S composites for
18 HPC/S-Sol-70% (D), HPC/S-155-70% (E), HPC/S-300-68% (F).

19
20
21
22
23 **Fig. 5.** TEM images of HPC (A), HPC/S composites for HPC/S-300-68% (B), HPC/S-
24 155-70% (C), HPC/S-Sol-70% (D) and corresponding elemental maps obtained by
25 EDX of the sulfur-filled porous carbon matrices (E-G).

26
27
28
29
30 **Fig. 6.** The cycling performances of the HPC/S composites at 200mA/g.

31
32 **Fig. 7.** Cyclic voltammograms of the HPC/S composites for HPC/S-Sol-70% (A),
33 HPC/S-155-70% (B), at a scan rate of 0.1 mV s⁻¹. Charge/discharge voltage profiles of
34 the (C) HPC/S-Sol-70%, HPC/S-155-70% (D), at first cycle of various C rates from
35 0.1C to 2C .

36
37
38
39
40
41
42
43 **Fig. 8.** The rate performances of HPC/S composites (A), the cycling performances of
44 the HPC/S-Sol-70% based on 7 mg cm⁻² s at 0.2 C and (B) the cycling performances of
45 the HPC/S composites at 1C (C).

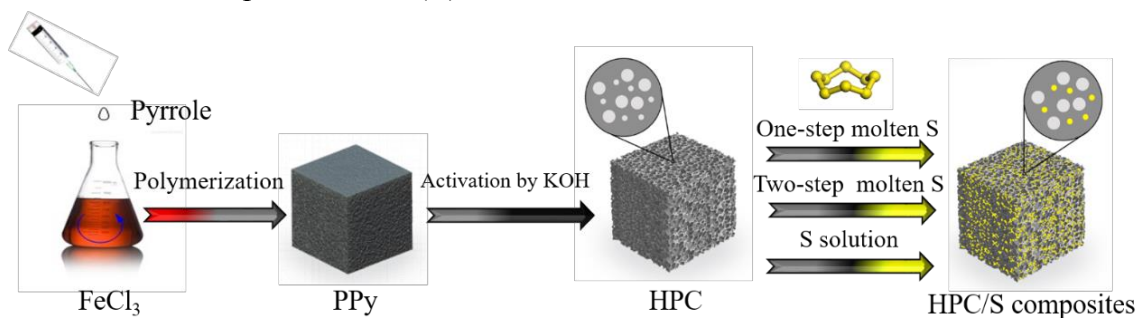


Fig. 1

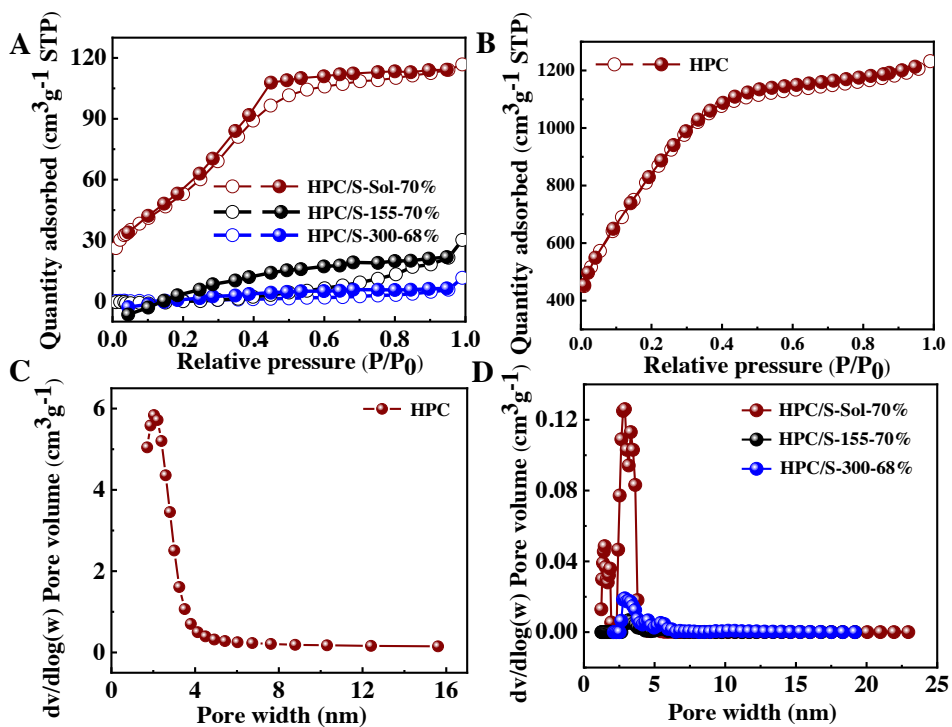


Fig. 2

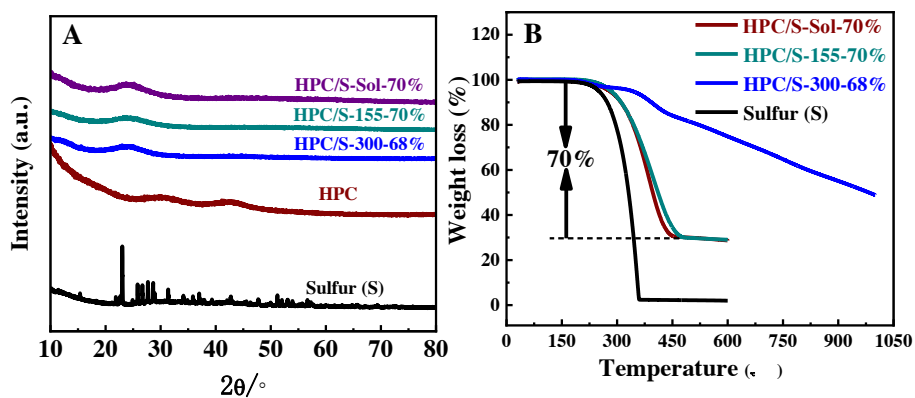


Fig. 3

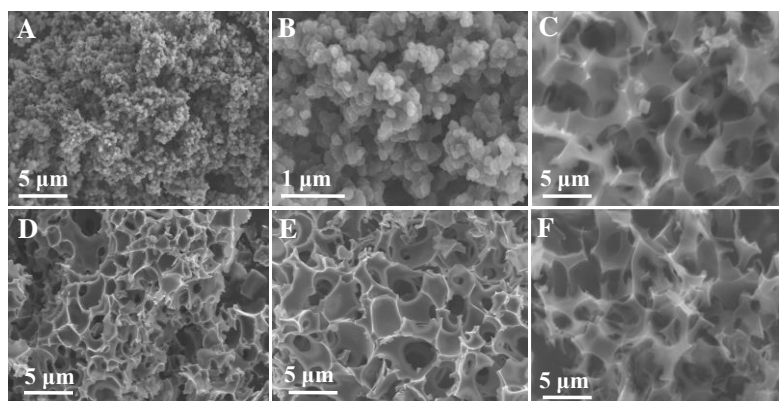


Fig. 4

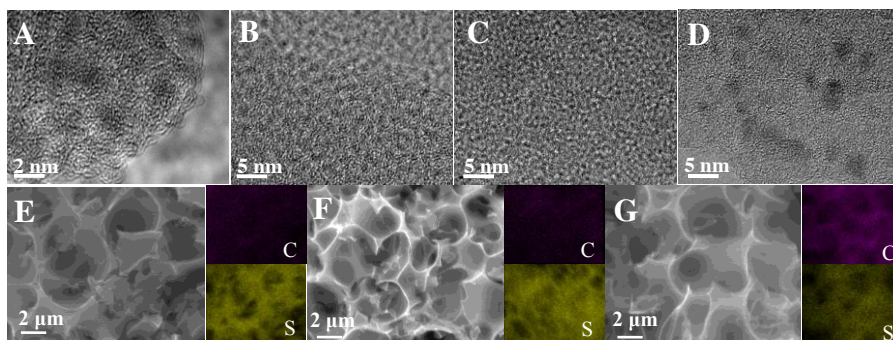


Fig. 5

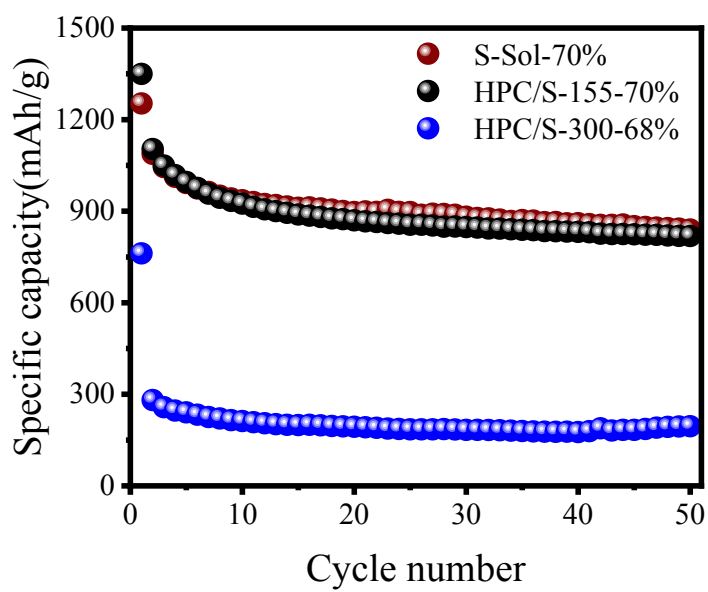


Fig. 6

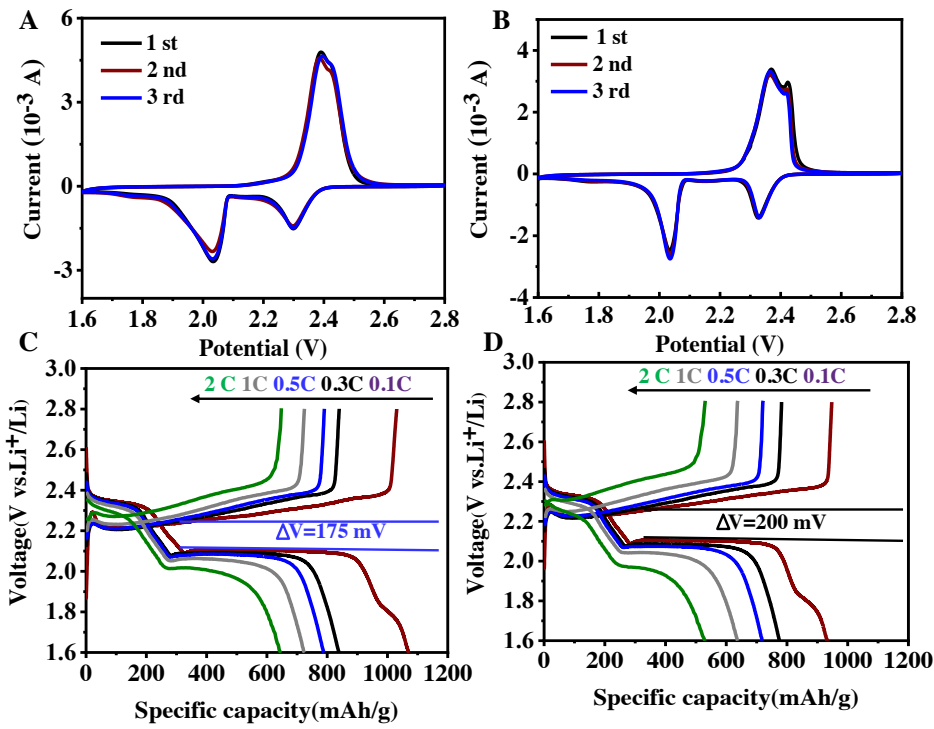


Fig. 7

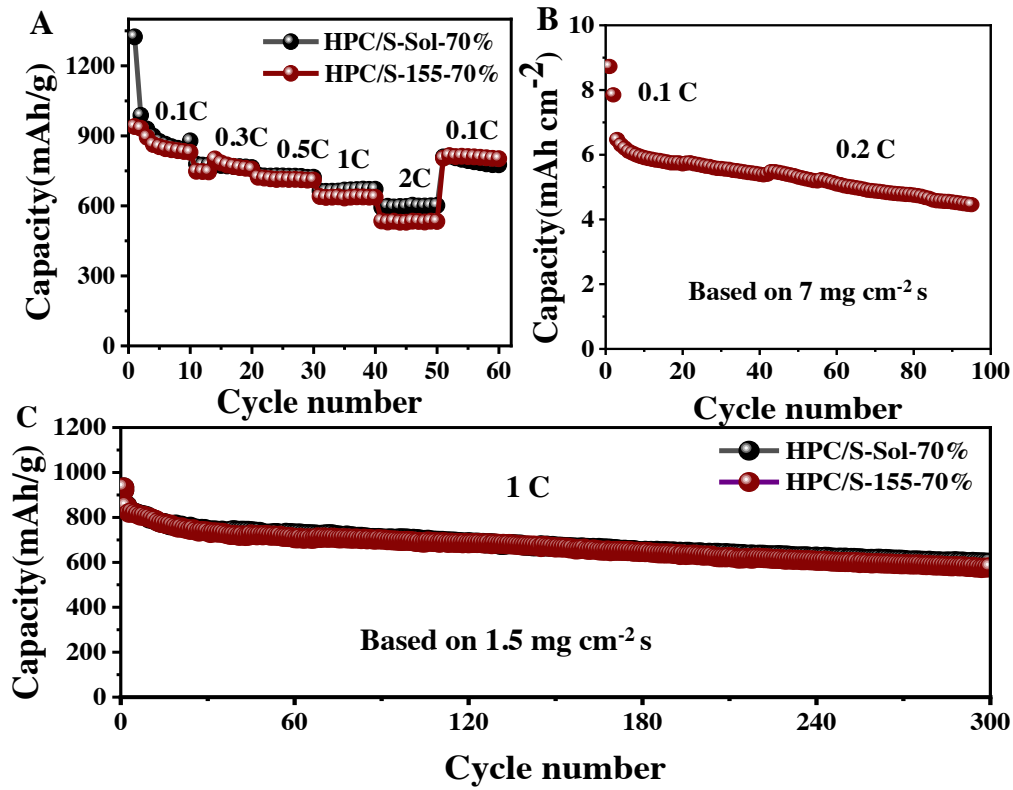


Fig. 8

1
2
3
4
5
6
7
8
9
10
11
12
13
14
15
16
17
18
19
20
21
22
23
24
25
26
27
28
29
30
31
32
33
34
35
36
37
38
39
40
41
42
43
44
45
46
47
48
49
50
51
52
53
54
55
56
57
58
59
60
61
62
63
64
65

Declaration of interests

The authors declare that they have no known competing financial interests or personal relationships that could have appeared to influence the work reported in this paper.

The authors declare the following financial interests/personal relationships which may be considered as potential competing interests:

Bo Zhang, Zhijie Guo, Yingming Zhao, Birong Luo , Dejun Li, Teng Zhao, Jagadeesh Sure, Sri Maha Vishnu, Amr Abdelkader, Chris Harris, Kai Xi

Authors' Replies to Reviewers' Comments

Dear Editor :

Thanks for your kind handling about our paper “*Effect of Loading Methods on the Performance of Hierarchical Porous Carbon/sulfur Composites in Lithium Sulfur Batteries*”. We greatly appreciate your tremendous efforts for the edition of our manuscript, and it is our great pleasure to receive the comments from you and the referees. The constructive comments and insightful suggestions from them are highly important for further improving the quality of our research. According to those comment and suggestion, we have revised the manuscript. The concerns have been carefully addressed and the mistakes have also been corrected in the revision. We sincerely hope this manuscript can be finally acceptable to be published in *Electrochimica Acta*.

The response to referees' comments

Reviewer # 1

Overall comment: This work reported hierarchical porous carbon/s cathode and compared the electrochemical performance of three different loading techniques. As the carbon based sulfur cathodes have been widely reported. The performance is not impressive and the novelty is poor. Therefore, I think this manuscript is not proper for the publication on *Electrochimica Acta*. Following are some concerns need to be addressed.

Response: Thank you very much for your comments and suggestions. We have made detailed modifications to the manuscript according to your suggestions. Although the three methods of loading sulfur are used in many literatures, they have not been systematically compared in hierarchical porous carbon. Therefore, we think our work is very meaningful.

Comment 1: There are a few typo errors in the manuscript and Figure.

Many thanks for your valuable suggestions. We've realized that the TEM & SEM images are incorrectly labelled. We have corrected the mistake.

Comment 2: The sulfur loading and sulfur content are very low.

Thanks very much for your suggestive comment. We've tested the high-load sulfur cells with a sulfur loading of 7 mg cm^{-2} . The HPC/S-Sol-70% electrode showed 4.4 mAh cm^{-2} after 98 cycles as shown in the following figure. Hence, with the reviewer's comments and suggestions, we have revised the corresponding part in the manuscript “Additionally, the HPC/S-Sol-70% composite cathode with 7 mg cm^{-2} sulfur areal loading also exhibited a high areal capacity of 8.7 mAh cm^{-2} at a current density of 0.1C and maintained a high areal capacity of 4.45 mAh cm^{-2} at a current density of 0.2C after 98 cycles (Figure 8b)”. According to your comments and suggestions, we have clarified this point in Page 15, Line 7-10.

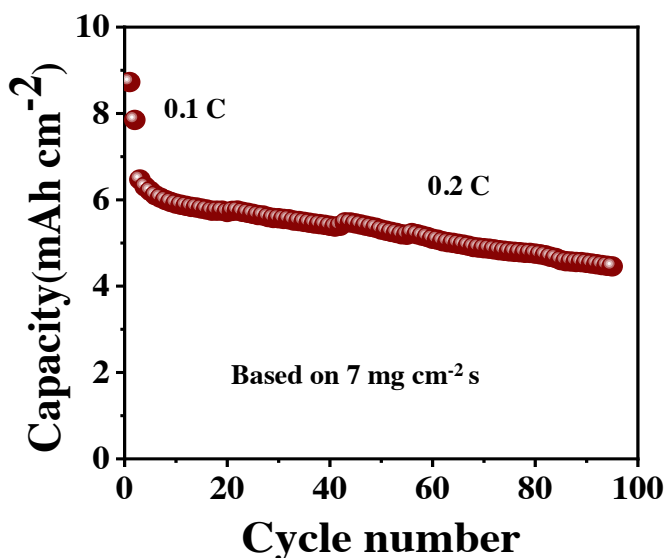


Fig. 8b. Cycling performance of the HPC/S-Sol-70% at 0.2C based on $7 \text{ mg cm}^{-2} \text{ s}$.

Comment 3: The cycling performance is not impressive.

Many thanks for your valuable suggestions. We've tested HPC/S-Sol-70%, HPC/S-155-70% again between 1.6-2.8 V at 1C as shown in the following figure. We have revised the corresponding part in the manuscript “The rate performances of the three composite cathodes were further investigated at various current densities from 0.1C to 2C . As can be seen from Fig. 8A, HPC/S-Sol-70% delivers reversible capacities of 1324.5, 778.9, 732.3, 663.5, 593.5 mAh g^{-1} at current densities of 0.1 C , 0.3 C , 0.5 C , 1 C , 2 C respectively, which are much higher than those of other HPC/composites.

When the current density is returned to 0.1C, the capacity is recovered to values of 809.5, 803.5, for the HPC/S-Sol-70%, HPC/S-155-70%, composites respectively. This again shows how the pore structures formed by the solvent-mediated loading method facilitated the utilization of sulfur.

The cycle performances of the three composites over 300 cycles at 1C between 1.6-2.8 V are shown in Fig. 8C. After 300 cycles, the discharge capacities of the two samples reach 599, 578.8 mAh g⁻¹ for HPC/S-Sol-70%, HPC/S-155-70% respectively. The HPC/S-Sol-70% composite cathode exhibited the best cycling performance, implying that the simple wet chemical synthesis route of deposition method contributes to a significant restriction of the shuttle effect for polysulfides.” According to your comments and suggestions, we have added this point in Page 14.

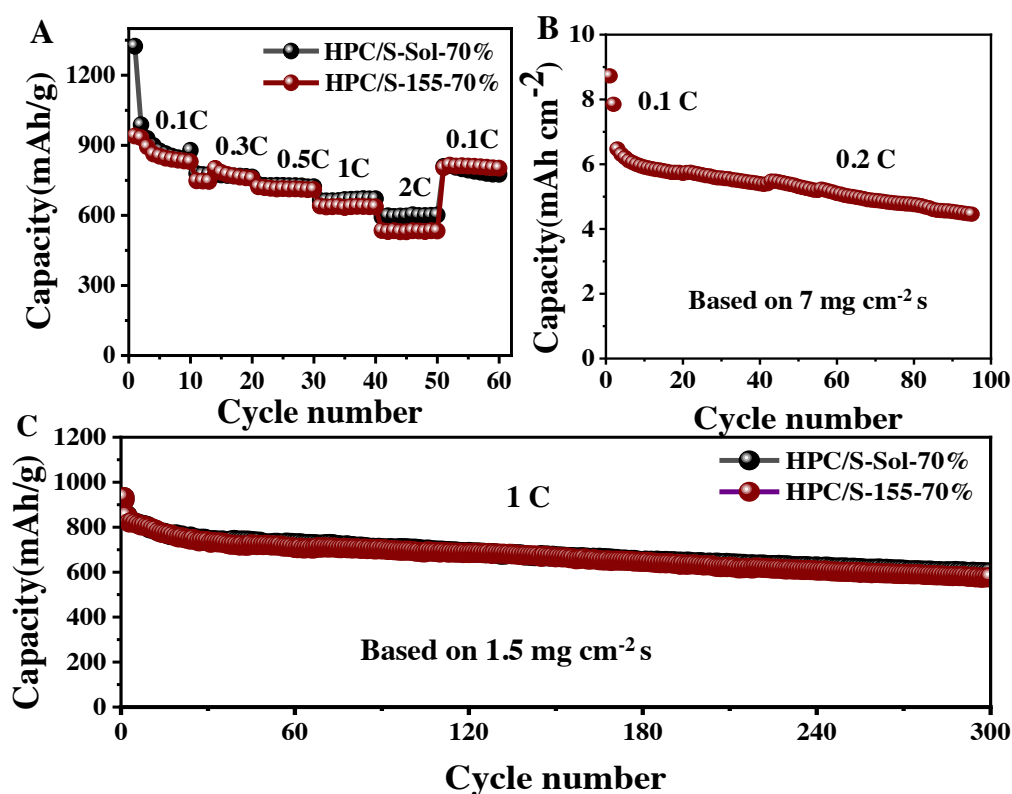


Fig.8. The rate performances of HPC/S composites (A), the cycling performances of the HPC/S-Sol-70% based on 7 mg cm⁻² s and (B) the cycling performances of the HPC/S composites at 1C (C).

Comment 4: The cycled electrode should be studied.

Many thanks for your valuable suggestions. We've researched the cycled electrode

and added in in the manuscript “After 100 cycles, the morphology of the positive electrode was tested. Compared with before cycling, there is little difference, and there is no large sulfur deposit (Figure S4).” According to your comments and suggestions, we have added this point in Page 15, Line 5-7.

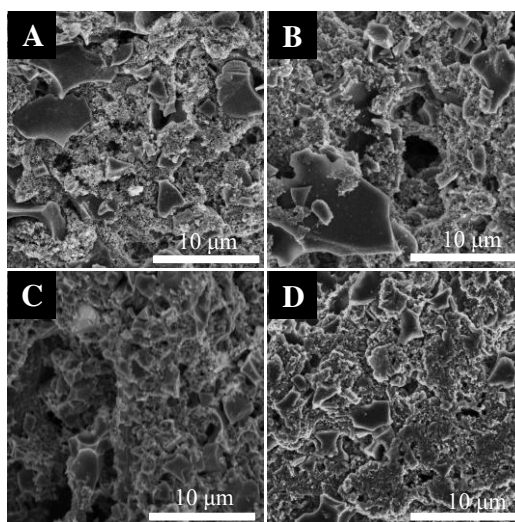


Fig. S4. SEM images of cathodes before cycling for HPC/S-Sol-70% (A), HPC/S-155-70% (C), and after one hundred cycles for HPC/S-Sol-70% (B), HPC/S-155-70% (D).

Comment 5: It is weird that the HPC/S-300 electrode shows poor electrochemical performance but has the lowest Rct.

Many thanks for your valuable suggestions. To confirm the result, we've re-tested electrochemical impedance spectroscopy and the HPC/S-300 electrode shows the highest Rct exactly. We have updated the EIS data in supporting information.

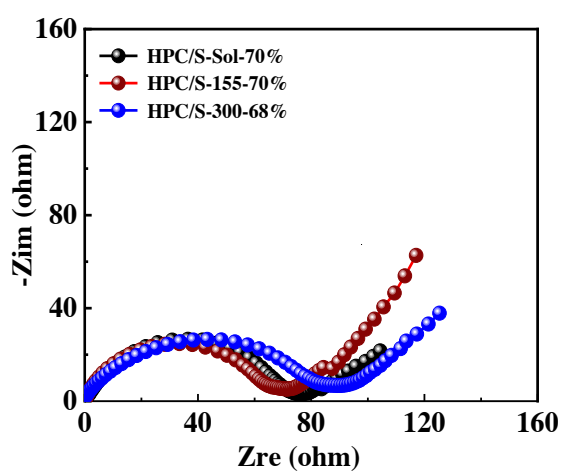


Fig. S3. Nyquist plots for the HPC/S composite cathodes before cycling.

Reviewer #2:

With the requirement of clean energy in modern everyday life, lithium-sulfur batteries become one of promising energy storage technologies. However, a couple of their drawbacks hinder their applications. In the manuscript "Effect of loading methods on the performance of hierarchical porous carbon/sulfur composites in lithium sulfur batteries", the authors adopted three loading approaches to prepare hierarchical porous carbon/ sulfur composite cathode, and found the "simple sulfur organic solution impregnation method" is the most effective approach to improve the electrochemical performance of the cathode. The morphologies and electrochemical performance of cathodes from different methods were examined. It is an interesting manuscript. However, I have some concerns.

Response: Thank you very much for the positive comments and recommendation on our research work. As the reviewer mentioned, our finding is an interesting study, and we try to provide an effect of loading method on the performance of hierarchical porous carbon/sulfur composites in lithium sulfur batteries, which can also inspire the broad interest in lithium sulfur batteries.

Comment 1: Please provide SEM images of cathodes from the three approaches after one hundred cycles.

Many thanks for your valuable suggestions. We've researched the cycled electrode and added in in the manuscript "After 100 cycles, the morphology of the positive electrode was tested. Compared with before cycling, there is little difference, and there is no large sulfur deposit (Figure S4)." According to your comments and suggestions, we have added this point in Page 15, Line 5-7.

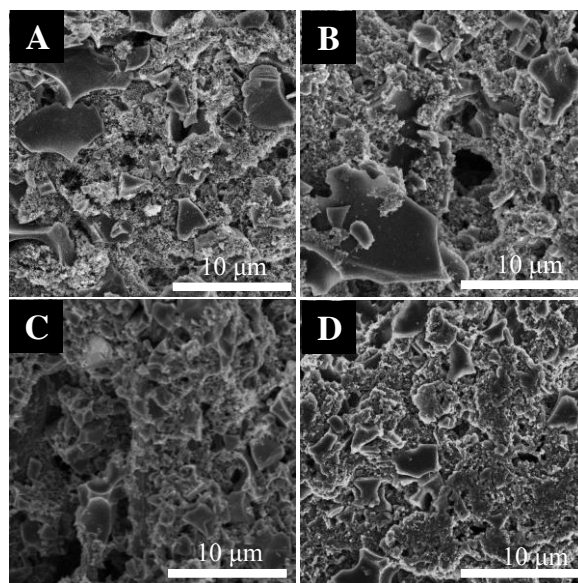


Fig. S4. SEM images of cathodes before cycling for HPC/S-Sol-70% (A), HPC/S-155-70% (C), and after one hundred cycles for HPC/S-Sol-70% (B), HPC/S-155-70% (D).

Comment 2: Figure 7: The cycle number is too small. Is it possible to provide a large cycle number for the discharge capacity.

Many thanks for your valuable suggestions. We've tested HPC/S-Sol-70%, HPC/S-155-70% again between 1.6-2.8 V at 1C as shown in the following figure. We have revised the corresponding part in the manuscript “The rate performances of the three composite cathodes were further investigated at various current densities from 0.1C to 2C. As can be seen from Fig. 8A, HPC/S-Sol-70% delivers reversible capacities of 1324.5, 778.9, 732.3, 663.5, 593.5 mAh g⁻¹ at current densities of 0.1C, 0.3C, 0.5C, 1C, 2C respectively, which are much higher than those of other HPC/composites. When the current density is returned to 0.1C, the capacity is recovered to values of 809.5, 803.5, for the HPC/S-Sol-70%, HPC/S-155-70%, composites respectively. This again shows how the pore structures formed by the solvent-mediated loading method facilitated the utilization of sulfur.

The cycle performances of the three composites over 300 cycles at 1C between 1.6-2.8 V are shown in Fig. 8C. After 300 cycles, the discharge capacities of the two samples reach 599, 578.8 mAh g⁻¹ for HPC/S-Sol-70%, HPC/S-155-70% respectively. The HPC/S-Sol-70% composite cathode exhibited the best cycling performance,

implying that the simple wet chemical synthesis route of deposition method contributes to a significant restriction of the shuttle effect for polysulfides.” According to your comments and suggestions, we have added this point in Page 14-15.

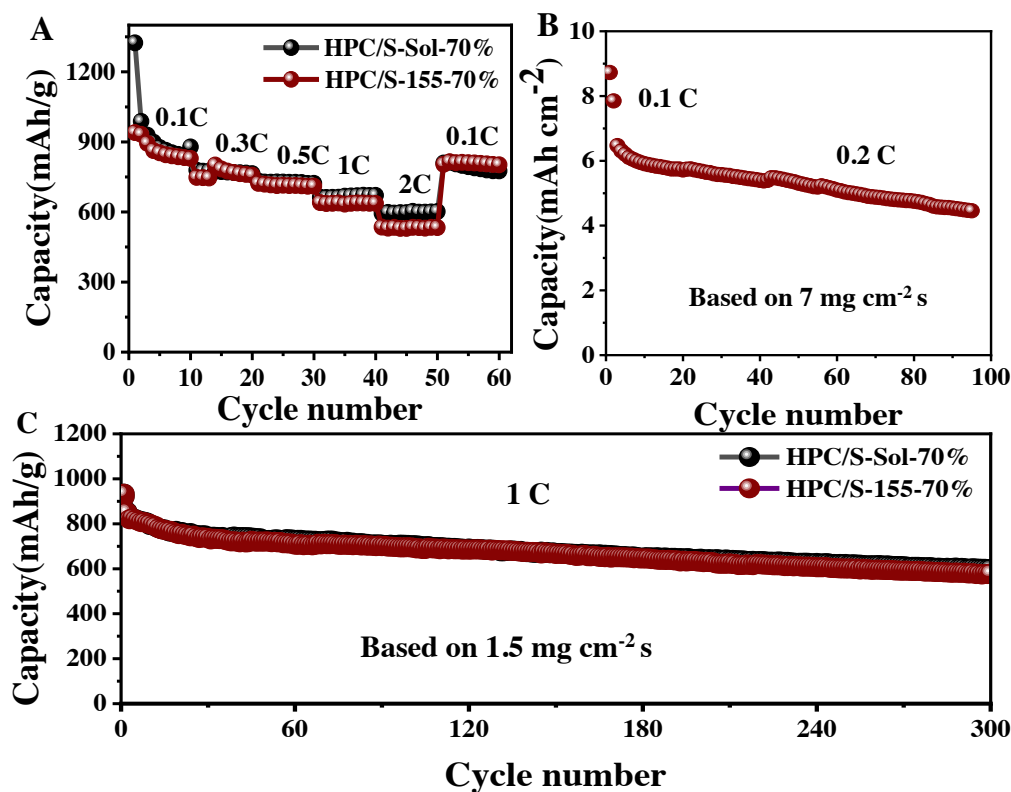


Fig.8. The rate performances of HPC/S composites (A), the cycling performances of the HPC/S-Sol-70% based on 7 mg cm⁻² s and (B) the cycling performances of the HPC/S composites at 1C (C).

Comment 3: The authors claim that the cathodes have good electrical conductivity. Can they prove it?

Thanks for your valuable suggestions. We have tested the electrical conductivity of the positive electrode with the four-probe method. The three cathodes have an electrical conductivity of 7–8 S cm⁻¹ at room temperature. “Despite nano-sized sulfur exists in the composite material, the three cathodes have an electrical conductivity of 7–8 S cm⁻¹ at room temperature.” We have added this point in Page 9 line16.

Comment 4: Introduction "Encapsulating sulfur into a conductive matrix has been

demonstrated to be an effective mean to confine polysulfide species and improve the electrical conductivity of the electrode. Various conductive matrixes have been explored, including porous carbon, carbon nanotubes, carbon nanofibers, graphene, and graphene derivatives, metal organic frameworks (MOFs) and metal oxides." More references (e.g. Journal of Materials Chemistry A, 2018, 6, 16574 -16582; Energy Storage Materials, 2019, 17, 118-125) are needed to support this statement.

Many thanks for your valuable suggestions. We have added the two references in the manuscript in Page 4, Line 6

[35] C. Zha, D. Wu, T. Zhang, J. Wu, H. Chen, Energy Storage Materials, 17 (2019) 118-125.

[36] C. Zha, F. Yang, J. Zhang, T. Zhang, S. Dong, H. Chen, Journal of Materials Chemistry A, 6 (2018) 16574-16582.

Comment 5: Section 2.2 "The HPC prepared form the previous step was used as the matrix..." Is it "from" or "form"?

Thanks very much for your suggestive comment. This is our mistake, we have correct it in the manuscript "The HPC prepared from the previous step was used as the matrix and sublimed sulfur (Aladdin, Shanghai) was used as the sulfur source"

Comment 6: Section 2.2 "For comparison, the graphene material obtained from Inner Mongolia RS new Energy Co., Ltd was incorporated with sulfur using the same three methods." Please provide the properties of the graphene materials adopted in this manuscript.

Many thanks for your valuable suggestions. We have added properties of the graphene materials in Page 6 line 22 (PH: 2 ± 0.2 ; N, S, Cl% $<0.5\%$; metal impurity <100 ppm; ash $<1.0\%$).

Comment 7: Section 3 "Also, the HPC possesses a relatively high total pore volume of $2.6 \text{ cm}^3 \text{ g}^{-1}$ and a large (BET) surface area of $3270.4 \text{ m}^2 \text{ g}^{-1}$ based on density function

theory calculation." Please provide the details of computational method and modeling of DFT.

Response:

The DFT models are created by classical approaches to adsorption as well as models based on modern statistical thermodynamics. Two simulation techniques are commonly used to determine the distribution of gas molecules in a system in equilibrium: the molecular dynamics method and the Monte Carlo method. Both of these are used as reference methods because their results are considered exact. We have added the details in page 8, line 18-20.

Reviewer #3:

This study looks at the impact of producing hierarchical material to produce a LSB. This is a good solid study, but more work is required to bring all of the pieces together. At present, one hypothesis is generated for each experimental observation, but the reader lacks one cohesive story at the end which draws all these components together. At some points there even seems to be conflicting findings.

Response: Thank you very much for the positive comments and recommendation on our research work. As the reviewer mentioned, our finding a good solid study, and we try to provide an effect of loading method on the performance of hierarchical porous carbon/sulfur composites in lithium sulfur batteries, which can also inspire the broad interest in lithium sulfur batteries.

For example, the CT resistance from the EIS for the HPC/S-300-68% cell is the lowest, but this cell performs very poorly. The current hypothesis provided is that the 300 cell has an excellent dispersion, but if this is the case, why does the cell perform so poorly in the battery testing? Also, this cell shows the highest over potential loss, which would suggest a low impedance.

Response: Many thanks for your valuable suggestions. To confirm the result, we've re-tested electrochemical impedance spectroscopy and the HPC/S-300 electrode shows the highest Rct exactly. We have updated the EIS data in supporting information

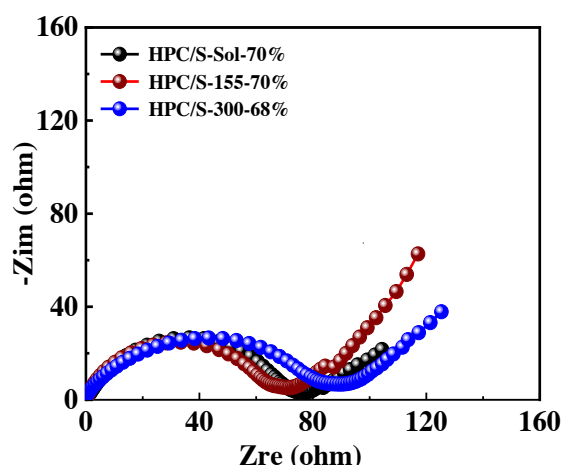


Fig. S3. Nyquist plots for the HPC/S composite cathodes before cycling.

From XRD it looks like you have a diffuse sulfur peak, this may simply suggest you have nano-sized sulfur and not amorphous sulfur.

Response: Thanks very much for your suggestive comment, after careful analysis and study, we have the same opinion with you. Some nano-sized sulfur exists in the composite material. We have added the corresponding part in the manuscript. "None of the HPC/S composites, regardless of the sulfur loading method, contain the characteristic peaks of crystalline sulfur, indicating that the nano-sized sulfur exists in the composite material." According to your comments and suggestions, we have added this point in Page 9, line 16-18.

Details missing from the SEM & TEM. Are these FEG instruments? If so, you would expect very low pressures. This could easily sublime the sulfur - especially in cases where the authors suggest that the sulfur is on the surface.

Response: Yes, these are FEG instruments for SEM and TEM with very low pressures, which can lead to some sublimation of the sulfur. However, this has almost no impact

on the SEM and TEM according to the obvious sulfur elemental maps obtained by EDX.

The TEM & SEM images are incorrectly labelled. Some images are labelled as TEM, but they are clearly SEM images. Can the authors please provide EDS point analysis data to check that the sulfur is being mapped. As stated above, sulfur easily sublimes, so it would be good to confirm that sulfur is being mapped and it isn't an artefact from another peak. It is not possible from these TEM images to confirm that sulfur is on the surface.

Response: We are sorry to make a mistake. We have corrected it carefully. And we also provided EDS point analysis data in supporting information according to the reviewer's suggestion, which can confirm that sulfur is on the surface of HPC accompanied with TEM images.

I cannot see any noticeable difference in the porous structures in the TEM images.

Response: It is almost indistinguishable from the observation on TEM, because the pore size is too small. We have modified the content in manuscript. The micropores and mesopores can be found out distinguishable from BET results.

I do not understand the argument presented on page 9 line 15 "The reason for the relatively ..." I am not sure what CS₂ solution is being referred to and why this leads to stretching and why this may lead to sulfur on the surface. If you have an opened structures, would you not expect more sulfur inside?

Response: Thanks very much for your suggestion. There is surface tension between the solution and the micropores, so that part of the sulfur cannot enter the pores. If all the elemental sulfur is in the micropores, the active material will not fully contact the electrolyte, resulting in increased polarization and incomplete utilization of the active material.

The key point of the paper the "hierarchical" structure seems to be brushed over in most of the discussions. Once again, this could be strengthened by drawing the findings

together more cohesively at the end of the paper. A schematic would help illustrate what your hypothesis is.

Response: Thanks for your suggestions. We have shown the "hierarchical" structure in the schematic of synthesis procedure of HPC and HPC/S. And the schematic was further modified based on your suggestions.

Why is a cut off voltage of 1 V used? This is very low for a LSB.

Response: Many thanks for your valuable suggestions. We've tested again between 1.6-2.8 V as shown in the following figure.

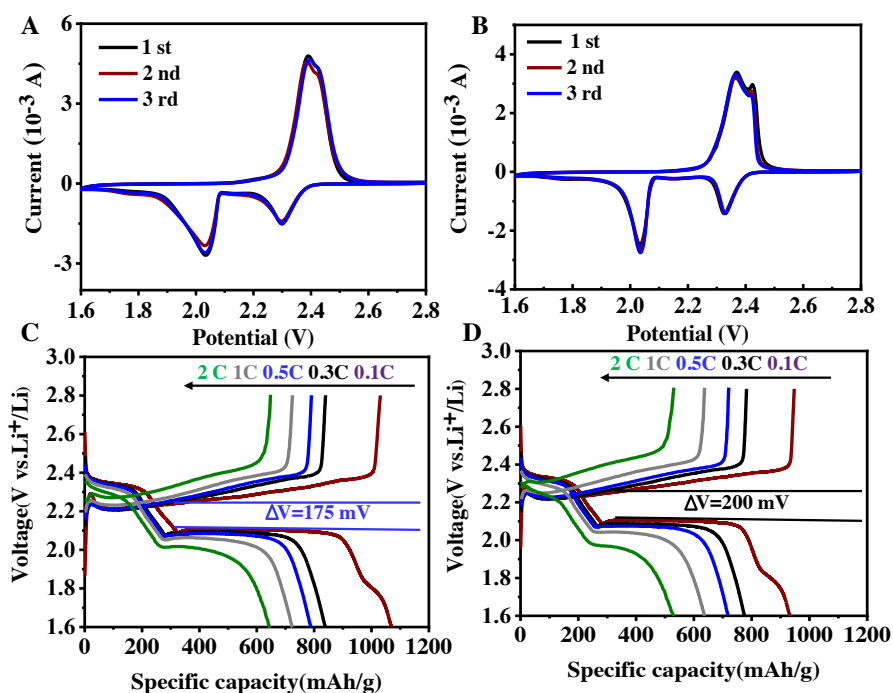


Fig. 7. Cyclic voltammograms of the HPC/S composites for HPC/S-Sol-70% (A), HPC/S-155-70% (B), at a scan rate of 0.1 mV s^{-1} . Charge/discharge voltage profiles of the (A) HPC/S-Sol-70% , HPC/S-155-70% (B), at first cycle of various C rates from 0.1C to 2C .

It is easier for the reader to have the sample labels directly on the images or graphs. For example in Figure 6 and the SEM and TEM images. Also as these figure labels are incorrect, I was really unsure what was being discussed.

Response: Many thanks for your valuable suggestions. We've realized that the TEM & SEM images are incorrectly labelled and corrected the mistake.

Although it is good to know the current density, please also include C-rates - this will be necessary to compare with other studies.

Response: Many thanks for your valuable suggestions. We've tested the properties of C-rates as shown in the following figure. The rate performances of the three composite cathodes were further investigated at various current densities from 0.1C to 2C. As can be seen from Fig. 8 A, HPC/S-Sol-70% delivers reversible capacities of 1324.5, 778.9, 732.3, 663.5, 593.5 mAh g⁻¹ at current densities of 0.1C, 0.3C, 0.5C, 1C, 2C respectively, which are much higher than those of other HPC/composites. When the current density is returned to 0.1C, the capacity is recovered to values of 809.5, 803.5, for the HPC/S-Sol-70%, HPC/S-155-70%, composites respectively. This again shows how the pore structures formed by the solvent-mediated loading method facilitated the utilization of sulfur.

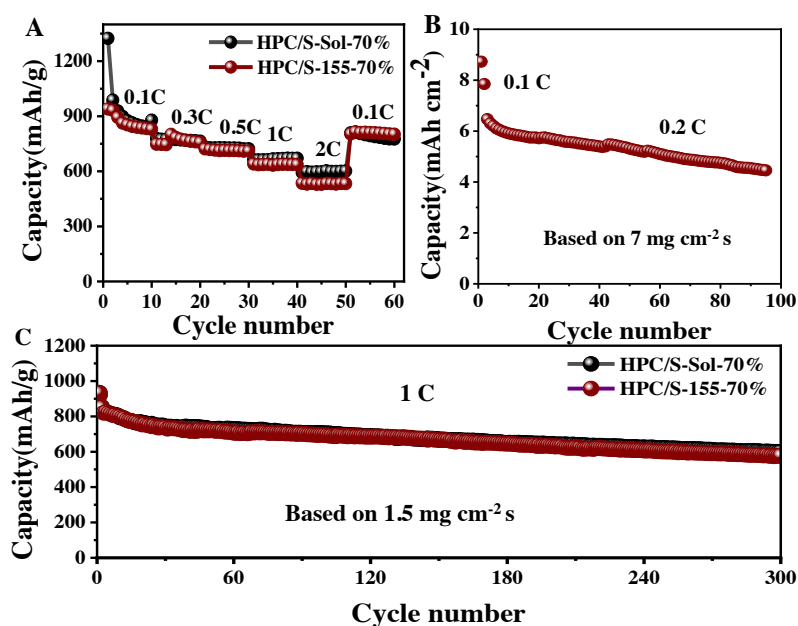
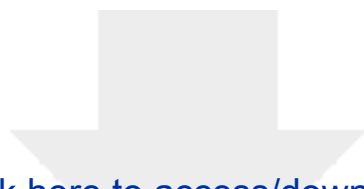


Fig.8. The rate performances of HPC/S composites (A), the cycling performances of the HPC/S-Sol-70% based on $7 \text{ mg cm}^{-2} \text{ s}$ and (B) the cycling performances of the HPC/S composites at 1C (C).



Click here to access/download
Supplementary Materials
supporting information-2021-3-31.docx

